Possible Sources of Trigger Mechanism of Electron-phonon Interactions in Doped CuTl-1223 Superconductors

Anila Kanwal (✉ anilakanwal2016@gmail.com)
  Quaid-i-Azam University Islamabad: Quaid-i-Azam University

Nawazish Ali Khan
  Quaid-i-Azam University Islamabad: Quaid-i-Azam University

Research Article

Loading [MathJax]/jax/output/CommonHTML/jax.js

Abstract

This article underlines the important role of copper Cu(3d^9) spins at the CuO$_2$ planer sites to comprehend the physics of High temperature Superconductivity . In such studies we have reported the characterization results of samples (Cu$_{0.5}$Tl$_{0.5}$)Ba$_2$Ca$_2$Cu$_3$O$_{10-\delta}$, (Cu$_{0.5}$Tl$_{0.5}$)(BaCa)(CaMg)Cu$_1$Zn$_2$O$_{10-\delta}$, (Cu$_{0.5}$Tl$_{0.5}$)(BaCa)(CaMg) Zn$_3$O$_{10-\delta}$ and (A$_y$Tl$_{1-y}$)(BaCa)(CaMg) Zn$_3$O$_{10-\delta}$ (A=Ag, K, Ni, Mn; y=0,0.5). Samples were prepared at normal pressure by using two-steps solid state reaction method. The characterization of samples is done via x-ray diffraction (XRD), resistivity (RT) and Fourier Transform Infrared (FTIR) absorption measurements. Intrinsic superconducting parameters and activation energy of all sample is estimated applying two theoretical models, Fluctuation Induced conductivity (FIC) analysis and Mott 3D-VRH. The XRD and FTIR absorption measurements have confirmed the intrinsic doping of K, Ag, Ni, Mn and Zn. Interestingly, samples (Cu$_{0.5}$Tl$_{0.5}$)(BaCa)(CaMg) Zn$_3$O$_{10-\delta}$ without CuO$_2$ planes have exhibited superconducting behavior above 77K. To verify the role of Cu(3d^9) atoms in superconductivity we have synthesized (A$_y$Tl$_{1-y}$)(BaCa)(CaMg) Zn$_3$O$_{10-\delta}$ (A=Ag, K, Mn, Ni; y=0,0.5) samples. In aforementioned samples, doping of Ni, Mn, K, Ag ions in Cu$_{1-x}$Tl$_x$Ba$_2$O$_{4-\delta}$ charge reservoir layer instead of Cu-atoms destroys the superconductivity completely and leads to semiconducting behavior. Key objective to preparing these samples is to investigate the role of two major parameters local moments (spin) of copper atoms and net carrier's concentration in superconductivity.

Introduction

In 1986 scientists found superconductivity in barium, lanthanum and copper oxide called La$_{1.85}$Ba$_{0.15}$CuO$_4$. The breakthrough awarded the scientists a Nobel Prize in Superconductivity and triggered a surge in condensed-mater physics research. Although similar oxides have revealed superconductors at temperatures as low as 30 K, Tc (transition temperatures) of later cuprates is almost an order of magnitude higher than any previously known superconductor [1−3]. In spite 33 years of research, no consent has arisen on causes of superconductivity in copper oxides [4−5]. As a result, main emphasis is on knowing the physical origin of the new Properties of the normal state in the expectation that these may provide significant insight into the advent of superconductivity at such high temperature. Cuprates are layered materials with a high anisotropy [6−7]. In oxides, superconductivity is found in CuO$_2$ planes and these planes are connected with charge reservoir layers which are separated by Ca atoms. In the oxide superconductor, the charge reservoir layer(CRL) sends charges to the superconduting plane (CuO$_2$) .The inter-plane coupling which is important in determining the magnitude of superconductivity arises from the correlation of carriers of different planes. The copper atoms in the CuO$_2$ planes have a small paramagnetic spin, which interacts with the carriers in conducting bands. The magnetic moments of nearly filled Cu^{2+}(3d ^{9}) have strong antiferromagnetic interactions with neighboring spin-½ Cu ions and each Cu atom is bound by an O ion [8−10]. Chemical doping is often used to change the charge concentration in the CuO$_2$ planes in order to explore the cuprate's unusual superconductivity. we will frame the discussion on two major parameters local moments(spin) and net carriers concentration. Here two questions arise. (1) Is there any contribution of spin of copper atoms (3d^9)? (2)Which factors enhance spin-spin interaction ? In current study we have synthesize (Cu$_{0.5}$Tl$_{0.5}$)(Ba$_2$Ca$_2$)Cu$_3$O$_{10-\delta}$ and Cu0.5Tl0.5(BaCa)(MgCa)ZnyCu3-yO10-δ (y = 2, 3) superconductors. In (Cu$_{0.5}$Tl$_{0.5}$)(BaCa)(CaMg)Zn$_3$O$_{10-\delta}$ sample we witnessed superconducting behavior even though Zn atoms, non-spin carrying entity with 3d^{10} state and mass almost equal to the Copper atom completely replace Cu-atoms in CuO$_2$ planar sites and make ZnO$_2$ plane. In the aforementioned sample superconductivity suppresses but it does not disappear, this trend arise a question and that is there any role of spin atom essential for the mechanism of superconductivity. To investigate the role of spin we replace spin carrying copper atom in charge reservoir layer Cu$_{0.5}$Tl$_{0.5}$(BaCa)O$_{4-\delta}$, by thallium atoms and synthesize (Tl$_{1.0}$)(BaCa)(CaMg)Zn$_3$O$_{10-\delta}$ sample in which copper Cu (3d^9) atom is transformed from CRL Tl$_{1.0}$(BaCa)O$_{4-\delta}$. Surprisingly sample turn semiconductor altogether. This result raised many questions.

To answer such questions and to investigate the role of local moments of impurity atoms (spins of copper) and net carriers concentration. We prepared samples by doping the charge reservoir layer with transition metals noble and Alkali metals.

Our technique for getting more knowledge is to replace copper atom Cu (3d^9) by others transition metal ions. In periodic table Nickle sit next to copper atom. So We synthesize (Ni$_{0.5}$Tl$_{0.5}$)(BaCa)(CaMg) Zn$_3$O$_{10-\delta}$ by replacing Copper atoms in charge reservoir layers Cu$_{0.5}$Tl$_{0.5}$(BaCa)O$_{4-\delta}$ by transition metals ions Ni(3d^8) substitution in the charge reservoir layer(CRL) again sample revealed semiconducting properties.

This arised other questions to be answered that is there any role of increase or decrease in effective magnetic moment per lattice site that disturbed the superconductivity?. In this scenario, we further prepared two samples (Mn$_{0.5}$Tl$_{0.5}$)(BaCa)(CaMg)Zn$_3$O$_{10-\delta}$ and (Ag0.5Tl$_{0.5}$)(BaCa)(CaMg) Zn$_3$O$_{10-\delta}$ by replacing Copper atoms in charge reservoir layers Cu$_{0.5}$Tl$_{0.5}$(BaCa)O$_{4-\delta}$ by transition metals ions Mn (3d^5)

Loading [MathJax]/jax/output/CommonHTML/jax.js

and Nobel Metal Ag. Astonishing no superconductivity was observed in such samples and it confirmed from results, superconductivity is only maintained in copper doped samples whereas doping with various d-Block elements (Tl, Ni, Mn, Ag) show semiconducting behavior.

Role of carrier concentration cannot be ruled out to study superconducting behavior. The copper atoms that are only present in CuO_2 planes are deficient in carriers and their spins are aligned antiferromagnetically, while charge reservoir layers have high carriers density. In order to enhance the density of charge carrier we prepared $(K_{0.5}Tl_{0.5})(BaCa)(CaMg)Zn_3O_{10-\delta}$ sample by replacing charge reservoir layers $Cu_{0.5}Tl_{0.5}(BaCa)O_{4-\delta}$ by this $K_{0.5}Tl_{0.5}(BaCa)O_{4-\delta}$ by substituting Potassium K on Copper sites. These samples with Alkali and Nobels metals also exhibited semiconducting variation of resistivity following Variable Range Hopping conductivity.

Experiment

These samples $(Cu_{0.5}Tl_{0.5})Ba_2Ca_2Cu_3O_{10-\delta}$, $(Cu_{0.5}Tl_{0.5})(BaCa)(CaMg)Cu_1Zn_2O_{10-\delta}$ and $(Cu_{0.5}Tl_{0.5})(BaCa)(CaMg)Zn_3O_{10-\delta}$ were prepared from solid state reaction technique completed in two stages using $Ca(NO_3)_2+4H_2O$, MgO, $Ba(NO_3)_2$, $Cu_2(CN)_2+H_2O$, ZnO. we also synthesized $(A_yTl_{1-y})(BaCa)(CaMg)Zn_3O_{10-\delta}$ (A=Ag, K, Ni, Mn; y=0,0.5)sample by two steps SSR method using $Ca(NO_3)_2+4H_2O$, MgO, $Ba(NO_3)_2$, ZnO, $Ni(NO_3)_2+H_2O$, MnO_2, $AgNO_3$, K_2CO_3 materials. Appropriate quantities of all high purity compounds is mixed, ground and sintered at 860 ^{o}C for 24 hours in a quartz boat with another intermediate grinding. Now in the twice fired material measured amount of Tl_2O_3 is mixed to get required compounds. The pressure of 3.8 tons/cm^2 is being used to pelletize these powder compounds. To reduce Tl losses, these pellets were individually wrapped in gold capsules and sintered at 860 ^{o}C for 10 minutes before being cooled to room temperature. X-ray diffraction was used to identify the material's crystal structure (XRD).The resistivity-temperature measurement is carried using four-probe method. (FTIR) Fourier Transform Infrared Spectroscopy measurements were used at ambient temperature to investigate phonon's modes.

Discussion And Results

Fig. 1(a) and Fig. 1(b) shows the X-ray spectra of $(Cu_{0.5}Tl_{0.5})Ba_2Ca_2Cu_3O_{10-\delta}$,$(Cu_{0.5}Tl_{0.5})(BaCa)(CaMg)Cu_1Zn_2O_{10-\delta}$, $(Cu_{0.5}Tl_{0.5})(BaCa)(CaMg)Zn_3O_{10-\delta}$ and $(A_yTl_{1-y})(BaCa)(CaMg)Zn_3O_{10-\delta}$ (A=Ag,K,Ni,Mn ;y=0,0.5) samples. The planar reflection of these samples corresponds to an orthorhombic crystal structure possessing Pmmm as space group. $BaCuO_2$ has a smaller number of impurity peaks, which has been revealed in diffraction scan. $BaCuO_2$ is a well-known stable chemical. It is produced by the decomposition of starting compounds through the decomposition of $Ba(NO_3)_2$ at early stages. The decomposed temperature of $Ba(CuO_2)$ is greater than thermally stable temperature of samples (~ 860°C), thus it stays in final compound's integral part. The variation of a and c-axis length is attributed to the fact that the ionic radius of Tl ions (1.48 A) is slightly greater than Cu, Ag Mn ions [11] shown in Table 1. In CuTl-1223 low intensity impurity peaks are detected in diffractogram. Structural changes can be seen in the final compound due to presence of different ionic radii.

Table 1
Shows the a-axis, b-axis, c-axis and volume values calculated from XRD analysis of $Cu_{0.5}Tl_{0.5}Ba_2Ca_2Cu_3O_{10-\delta}$ and $Cu_{0.5}Tl_{0.5}(BaCa)(MgCa)Zn_yCu_{3-y}O_{10-\delta}$ (y = 2, 3) superconductors and of $(A_yTl_{1-y})(BaCa)(CaMg)Zn_3O_{10-\delta}$ (A=Ag, K, Ni, Mn; y= 0,0.5) samples

S/N	Sample	a-axis (Å)	b-axis (Å)	c-axis (Å)	Volume(A^3)
$Cu_{0.5}Tl_{0.5}Ba_2Ca_2 Cu_3O_{10-\delta}$	3.83	3.81	14.44	207	
$Cu_{0.5}Tl_{0.5}(BaCa)(MgCa)Zn_2Cu_1O_{10-\delta}$	3.84	3.82	14.57	213	
3	$Cu_{0.5}Tl_{0.5}(BaCa)(MgCa)Zn_{3.0}O_{10-\delta}$	3.96	3.91	14.83	225
4	$Tl_{1.0}(BaCa)(MgCa)Zn_{3.0}O_{10-\delta}$	3.50	3.82	14.11	188
5	$K_{0.5}Tl_{0.5}(BaCa)(MgCa)Zn_{3.0}O_{10-\delta}$	3.72	3.83	14.04	198
6	$Ag_{0.5}Tl_{0.5}(BaCa)(MgCa)Zn_{3.0}O_{10-\delta}$	3.70	3.74	14.03	196
7	$Ni_{0.5}Tl_{0.5}(BaCa)(MgCa)Zn_{3.0}O_{10-\delta}$	3.71	3.77	14.10	200
8	$Mn_{0.5}Tl_{0.5}(BaCa)(MgCa)Zn_{3.0}O_{10-\delta}$	3.69	3.70	14.07	197

Loading [MathJax]/jax/output/CommonHTML/jax.js

Fig. 2(a) show temperature dependence of resistivity plots of $(Cu_{0.5}Tl_{0.5})Ba_2Ca_2Cu_3O_{10-\delta}$, $(Cu_{0.5}Tl_{0.5})(BaCa)(CaMg)Cu_1Zn_2O_{10-\delta}$ and $(Cu_{0.5}Tl_{0.5})(BaCa)(CaMg)Zn_3O_{10-\delta}$ samples. These samples exhibited superconducting metallic variations of resistivity from room temperature down to (R=0) and have Tc around 100.2, 92 and 91 K, Tc (onset) 113,108,119 K respectively shown in Table 2. As demonstrated in Fig. 2(b,c,d,e,f), all samples $(A_yTl_{1-y})(BaCa)(CaMg)Zn_3O_{10-\delta}$ (A=Ag,K,Ni,Mn ;y=0,0.5) have semiconductor-like resistivity variations with temperature.

Table 2
Shows the parameters T_c[onset] and T_c[R=0] calculated from resistivity vs. temperature graphs of $Cu_{0.5}Tl_{0.5}Ba_2Ca_2Cu_3O_{10-\delta}$ and $Cu_{0.5}Tl_{0.5}(BaCa)(MgCa)Zn_yCu_{3-y}O_{10-\delta}$ (y = 2, 3) superconductors.

Sample	T_c [R=0] (K)	T_c [onset] (K)
$Cu_{0.5}Tl_{0.5}Ba_2Ca_2 Cu_3O_{10-\delta}$	100.2	113
$Cu_{0.5}Tl_{0.5}(BaCa)(MgCa)Zn_2Cu_1O_{10-\delta}$	92	108
$Cu_{0.5}Tl_{0.5}(BaCa)(MgCa)Zn_{3.0}O_{10-\delta}$	91	119

Various models have been used to characterize electrical properties; the conduction process is guided by charge carriers hopping between levels via different methods. In many disordered carbon forms for charge carriers the Mott variable range hopping (VRH) and thermally assisted hopping are suggested as probable conduction mechanisms [12−13]. Eqn (1) gives the Mott VRH model, which is based on charge carriers hopping between localized states near the Fermi level with the assist of thermal energy. To is the characteristic hopping temperature while factor (ρ_o) is temperature T dependent.

$$\rho(T) = \rho_o exp\left[\left(\frac{T_0}{T}\right)^{1/4}\right] \qquad (1)$$

Due to the randomization in the conduction channels, carrier transport is actually proceeds via three-dimensional (3D) variable range hopping process. As a result using the Mott 3D VRH type conduction mechanism (equation (1), b = 1/4) [14−15] the ρ−T data of the various samples was evaluated. The Mott 3D VRH model remains in good fit for the experimental data of our samples. All samples $(A_yTl_{1-y})(BaCa)(CaMg)Zn_3O_{10-\delta}$ (A=Ag,K,Ni,Mn ;y=0,0.5)) have semiconductor-like resistivity variations with temperature fitted by equation 1 in the temperature regime from 77K to 300K shown in Fig. 3(a,b,c,d,e). The inset represents the plot of ln $\varvec{\rho}$ vs. $1/T^{1/4}$, where the theoretical prediction for the Mott Varying Range Hopping (VRH) in 3D mechanism is indicated by the straight line. The energy of activation for $Tl_{1.0}(BaCa)(CaMg)Zn_3O_{10-\delta}$, $Tl_{0.5}Ag_{0.5}(BaCa)(CaMg)Zn_3O_{10-\delta}$, ,$Tl_{0.5}K_{0.5}(BaCa)(CaMg)Zn_3O_{10-\delta}$, $Tl_{0.5}Ni_{0.5}(BaCa)(CaMg)Zn_3O_{10-\delta}$, and $Tl_{0.5}Mn_{0.5}(BaCa)(CaMg)Zn_3O_{10-\delta}$, sample is 1.85meV, 1.41meV, 2.35meV, 2.34 meV and 6.89 meV respectively as shown in Table 3.

Table 3
Activation energy of $(A_yTl_{1-y})(BaCa)(CaMg) Zn_3O_{10-\delta}$ (A=Ag, K, Ni, Mn; y= 0,0.5) samples

Sample	Activation Energy Ea(meV)
$K_{0.5}Tl_{0.5}(BaCa)(MgCa)Zn_{3.0}O_{10-\delta}$	2.35
$Ag_{0.5}Tl_{0.5}(BaCa)(MgCa) Zn_{3.0}O_{10-\delta}$	1.41
$Tl_{1.0}(BaCa)(MgCa) Zn_{3.0}O_{10-\delta}$	1.85
$Mn_{0.5}Tl_{0.5}(BaCa)(MgCa) Zn_{3.0}O_{10-\delta}$	6.89
$Ni_{0.5}Tl_{0.5}(BaCa)(MgCa) Zn_{3.0}O_{10-\delta}$	2.34

We observed superconductivity in $(Cu_{0.5}Tl_{0.5})(BaCa)(CaMg) Zn_3O_{10-\delta}$ sample without CuO_2 plane. As we know charge reservoir layer $Cu_{0.5}Tl_{0.5}(BaCa)O_{4-\delta}$ supply carriers to the superconducting planes CuO_2 plane as Cu-atom from CRL jump to ZnO_2 planar sites and their presence both in Superconducting plane and charge reservoir layer produce spin fluctuation and disturb Anti-ferromagnetic order. In order

Loading [MathJax]/jax/output/CommonHTML/jax.js

to verify the role of copper spin ($3d^9$) we prepared $(A_yTl_{1-y})(BaCa)(CaMg)Zn_3O_{10-\delta}$ (A= Ni, Mn, Ag, K; y=0,0.5) samples, main objective to prepare these samples is to completely remove copper from the charge reservoir layer $Cu_{0.5}Tl_{0.5}(BaCa)O_{4-\delta}$ and superconducting planes CuO_2. In such samples Cu-based CRL is exchanged by $Tl_{1.0}(BaCa)O_{4-\delta}$, $Ni_{0.5}Tl_{0.5}(BaCa)O_{4-\delta}$, $Mn_{0.5}Tl_{0.5}(BaCa)O_{4-\delta}$, $Ag_{0.5}Tl_{0.5}(BaCa)O_{4-\delta}$ and $K_{0.5}Tl_{0.5}(BaCa)O_{4-\delta}$. As all CRL layers are conducting, none of them possess a spin-carrying particle like Cu($3d^9$). As a result, such charge reservoir layers eliminate the possibility of Cu-atoms diffusing to CuO_2-planar positions. As a result, all samples without copper atoms in the CRL have exhibited semiconducting conductivity with different activation energy.

As copper Cu($3d^9$) is transitional metal, we replace copper atoms from CRL by another d-element nickel Ni($3d^8$) that is ferromagnetic entity [16] that can supply alternatively larger spin as compared to Cu($3d^9$) atoms of CRL $Cu_{0.5}Tl_{0.5}(BaCa)O_{4-\delta}$. In $(Ni_{0.5}Tl_{0.5})(BaCa)(CaMg) Zn_3O_{10-}$ sample we increase interplanar coupling by doping Mg atoms at Calcium sites and in CRL $Cu_{0.5}Tl_{0.5}(BaCa)O_{4-\delta}$ replace copper atoms with Ni($3d^8$). Results have shown that with Ni-doping we obtain semiconducting behavior. Now we prepare another sample $(Mn_{0.5}Tl_{0.5})(BaCa)(CaMg) Zn_3O_{10-\delta}$ by doping d-element Mn($3d^6$) in charge reservoir layer. To enhance magnetic moment per lattice cell we substitute Mn in charge reservoir layer (CRL) $Mn_{0.5}Tl_{0.5}(BaCa)O_{4-\delta}$. As superconducting planes are deficient of carriers and there is antiferromagnetic alignment of spin when Mn is substituted in (CRL) $Mn_{0.5}Tl_{0.5}(BaCa)O_{4-\delta}$ it induce no superconducting transition and the sample obeyed semiconducting behavior. Mn is a magnetic impurity that causes pairs breaking; hence no superconductivity might be expected.

We synthesize further sample $(Ag_{0.5}Tl_{0.5})(BaCa)(CaMg) Zn_3O_{10-\delta}$ by doping Ag($4d^{10}$) in CRL $Ag_{0.5}Tl_{0.5}(BaCa)O_{4-\delta}$ plane. The idea to doped Nobel metal instead of Cu($3d^9$) to check is there any significance of spin carrying entity in the mechanism of superconductivity at high temperature? Such samples have shown semiconducting behavior.

To investigate the role of the density of charge carrier we synthesize $(K_{0.5}Tl_{0.5})(BaCa)(CaMg) Zn_3O_{10-\delta}$ using Alkali Metal so potassium K($4s^1$) is introduced in charge reservoir layer. K is substituted in CRL $K_{0.5}Tl_{0.5}(BaCa)O_{4-\delta}$ to increase density of charge carriers in superconducting plane Cu/ZnO_2. Even the deliberate enhancement in the carrier density Via K-doping at charge reservoir layer sites have not given us superconductivity down to 77K instead produce semiconducting samples.

All such studies have revealed some of Cu-atoms in the CRL $Cu_{0.5}Tl_{0.5}(BaCa)O_{4-\delta}$ most likely hop to the ZnO_2 planes. This shows the significance of spin carrying Cu($3d^9$) atoms in the plane that cause fluctuating in spin and produce spin density wave. These spin fluctuation seem to mediate long range phase coherence established superconductivity at Tc. In cuprates spin of copper atom play vital role in superconductivity. While all samples $(A_yTl_{1-y})(BaCa)(CaMg)Zn_3O_{10-\delta}$ (A=Ag,K,Ni,Mn ;y=0,0.5) without Copper atoms show semiconducting behavior which supports our thesis that in the absence of a copper atom, electron spins flip on varying degree that causes scattering waves asymmetrically that in turn disturb coherence in wave function. This process disrupts phase coherence, resulting in destructive interference, which leads to an increase in resistivity [17−19].

Conventional superconductors possess *s*-wave symmetry and are isotropic. Cooper pairing of electrons is mediated by lattice phonons. While in cuprates the superconducting wavefunction possesses d-wave symmetry, which means it changes sign when rotated by 90°[20-21]. When a cuprate is doped, the charge carriers delocalize due to hybridization between the Cu (3d) and O (2p) orbitals. Still, it's unclear what causes the material to superconductor at some critical doping levels. The pairing mechanism may be initiated by superexchange phenomena, in which spin fluctuations between neighboring Cu sites are mediated by O atoms that partition the Cu atoms. The Cu ($d_{x^2-y^2}$) orbital's energy is almost degenerate with those of O(2p) orbitals in cuprates, making hybridization and hence spin fluctuation extremely strong. The energy levels of the Ni, Ag, K, Mn, and O orbitals, on the other hand, are quite different, weakening the spin fluctuations [22−23].

Aslamazov and Larkin [24] used a microscopic technique to calculate excess conductivity where the fluctuation are modest. They derived $\sigma /\sigma 300 = A\varepsilon^\lambda$ (1) with reduced temperature $\varepsilon = (T - Tmf)/ Tmf$ (mean field temperature Tmf is calculated from peak of $d\rho/dT$ against T plot). The Lawrence and Doniach (LD) model for the polycrystalline samples, is as follow [25].

$$\Delta\sigma_{LD} = [e^2/ (16\hbar d)](1+J\varepsilon^{-1})^{-1/2}\varepsilon^{-1} \quad (2)$$

In the preceding expression $J= [2\xi_{c(0)}/d]^2$ represent inter-CuO_2-layers couplings, d signifies thickness of superconducting layers and the coherence length $\xi_{c(0)}$ is along c-axis. By using LD model the coherence length is determined from the crossover temperatures by

Loading [MathJax]/jax/output/CommonHTML/jax.js ples [26].

$\xi_{c(0)} = d/2[(T_{3D-2D}/T_{mf})-1]^{1/2}$ (3)

$\ln(\sigma)$ was plotted against $\ln(\varepsilon)$ in Fig. 4(a,b,c) to analyze the excess conductivity applying AL model. This can be seen, each plot is categorized into three distinct regions. The different sections of the plots are linearly fitted and exponent values 'λ' is derived from the slopes to relate the experimental results with theoretical values. The λcr (critical exponent) corresponds to the critical region has a value of 0.33, λ_{3D} values ranging from -0.48 to -0.564 showing 3D behavior, λ_{2D} values ranging -0.92 to -1.0089 signifying 2D behavior see in Table 4. In afore mentioned samples Mg-atoms are substituted at Ca sites, in prior research Ca by Mg atoms were successfully replaced, that suppresses c-axis length and rise critical current density [27]. The critical temperature does not rise in $(Cu_{0.5}Tl_{0.5})(BaCa)$ $(CaMg)$ $(Cu_{3-x}Zn_x)O_{10-d}$ (x = 2,3) samples indicating that the $Zn(3d^{10})$ cause disorder in antiferromagnetic aligned of copper atoms($3d^9$) spins within CuO_2 plane. Because of disturbance in the spin density waves (SDW) charge stripes are likely to reorder, lead to suppressing superconductivity.

Table 4
Shows widths of critical, 3D, 2D, and 0D fluctuation regions observed from

Sample	λ_{CR}	λ_{3D}	λ_{2D}	λ_{0D}	$T_{CR-3D} = T_G$ (K)	T_{3D-2D} (K)	T_{2D-0D} (K)	T_c^{mf} (K)	T^* (K)	$\alpha = \rho_n(0K)$ (Ω-cm)
y=0	0.30	0.53	1.0	2.0	106	109	112	101.8	136	0.45
y = 2	0.33	0.5	1.2	2.0	102.5	105	110	97.5	129	0.40
y = 3.0	0.32	0.51	1.1	2.0	104	108	112	100.2	140	2.1

We elucidated important superconducting parameters using Ginzburg Landau theory and equation stated in our earlier articles [28-30]. The parameters like $J_c(0)$, $B_{c(0)}$, $B_{c1(0)}$, $B_{c2(0)}$, and κ = λ/ξ are computed for $(Cu_{0.5}Tl_{0.5})Ba_2Ca_2Cu_3O_{10-\delta}$ and $(Cu_{0.5}Tl_{0.5})(BaCa)(CaMg)$ $(Cu_{3-x}Zn_x)O_{10-\delta}$ (x = 2, 3) samples, shown in Table 5. In our samples the values of $J_c(0)$,$B_{c0}(T)$, $B_{c1}(T)$ suppressed. The number of unintended defects, calculated by parameter α in samples enhanced with increasing Zn-doping, decrease in $B_{c(0)}$, $B_{c1(0)}$, $B_{c2(0)}$, $J_c(0)$ values indicate that these defects are not behaving as pinning centers. Table 5 shows that the London penetration depth $\lambda_{p.d}$ and the GL parameter increase in all doped samples.

Table 5
Shows the superconductivity parameters observed from the FIC analysis of $Cu_{0.5}Tl_{0.5}Ba_2Ca_2Cu_3O_{10-\delta}$ and $Cu_{0.5}Tl_{0.5}$ (BaCa) $(MgCa)Zn_yCu_{3-y}O_{10-\delta}$ (y = 2, 3) superconductors.

Sample	$\xi_c(0)$ (Å)	J	N_G	$\lambda_{p.d}$ x 10^2 (Å)	B_{c0} (T)	B_{c1} (T)	B_{c2} (T)	κ	$J_{c(0)}$ x 10^3 (A/cm^2)	V_F x 10^7 (m/s)	E_{Break} (eV)	τ_φ x 10^{-13} (s)
y=0	2.090	0.077	0.048	846.87	1.716	0.089	127.70	51.99	1.099	1.797	0.0198	2.0529
y = 2	2.140	0.080	0.052	914.09	1.593	0.077	127.70	58.19	0.941	1.705	0.0293	1.40394
y = 3.0	2.26	0.091	0.051	985.92	1.475	0.068	127.70	62.55	0.812	1.769	0.0351	1.18929

The phonon modes are observed in order to understand the process of high temperature superconductivity because electron-phonon interactions are probably important for superconductivity's mechanism. Oxygen, have highest vibrational amplitude due to its smaller atomic size, is responsible for causing such electron phonon interactions. In the CuTl-1223 unit cell, oxygen phonon modes have been witnessed (above 400 cm^{-1}). The infrared absorption bands between 50 and 350 cm^{-1} in layered cuprate superconductors are thought to be caused by the vibration of Tl ,Cu, Ca and Ba atoms, whereas the absorption bands above 400 cm^{-1} are considered to be caused by the vibration of lighter oxygen atoms of chain, planer, and apical oxygen. Two apical oxygen atoms of type $Tl-O_A-Cu(2)$ and $Cu(1)-O_A-Cu(2)$ are witnessed around 420−460, 480−540 cm^{-1}, Cu(2) atom is in superconducting plane and Cu(1) atom in charge reservoir layer(CRL). CuO_2 planar oxygen mode is witnessed around 550−580 cm^{-1} [31-33]. FTIR measurements of our $Cu_{0.5}Tl_{0.5}Ba_2Ca_2Cu_3O_{10-\delta}$, $(Cu_{0.5}Tl_{0.5})$ $(BaCa)(CaMg)Cu_1Zn_2O_{10-\delta}$ and $Cu_{0.5}Tl_{0.5}(BaCa)(CaMg)Zn_3O_{10-\delta}$ samples shown in Fig. 5(a). CuO_2 planar mode continuously softened

Loading [MathJax]/jax/output/CommonHTML/jax.js

with increasing Zn doping finally attain 515 cm^{-1} in $(Cu_{0.5}Tl_{0.5})(BaCa)(CaMg)Zn_3O_{10-\delta}$ samples. Although the apical oxygen bond length increases, the influence of the mass of Zn atoms is obvious in softening of these modes, which is most likely connected with the greater mass of Zn (65.38amu) atoms in contrast to Cu(63.54amu) atoms. The addition of Zn-atoms at Cu sites in the CuO_2 plane is indicated in the variation of modes.

From Fig. 5(b,c), FTIR absorption measurements of samples $(A_yTl_{1-y})(BaCa)(CaMg)Zn_3O_{10-\delta}$ (A=Ni, K, Ag, Mn ; y=0,0.5) the phonon's modes associated to the vibrations of different oxygen atoms have been observed between $400-700$ cm^{-1}. Presence of modes at some different wavenumber as compared to CuTl-1223 system can be attributed to the modified layer of charge reservoir layer $Cu_{0.5}Tl_{0.5}(BaCa)O_{4-\delta}$. Although the position of modes is determined from the bonding among attached atoms. The larger sizes atom of thallium Tl (1.4 A^o) in the charge reservoir layer (CRL) $Tl_{0.5}Tl_{0.5}(BaCa)O_{4-\delta}$ possibly increase the size of a-axis. The central presence of Tl^{3+} in CRL shows high stability of O-atom. Thallium content in the CRL make it insulating and in the superconducting layer free carriers concentration decrease. Since Thallium is a heavy atom its modes has lowest energy and apical oxygen modes move toward lower wavenumber. In $Tl_1(BaCa)(CaMg)Zn_3O_{10-\delta}$ sample both apical oxygen modes of type $Tl-O_A-Zn(2)$ are witnessed about 486 cm^{-1} and 521 cm^{-1}.

We prepared $Ni_{0.5}Tl_{0.5}(BaCa)(CaMg)Zn_3O_{10-\delta}$ and $K_{0.5}Tl_{0.5}(BaCa)(CaMg)Zn_3O_{10-\delta}$ samples. When we doped CRL with heavy atoms like Ni(1.62 A^o) and K(2.03 A^o) the apical oxygen modes of type $Tl-O_A-Zn(2)$ slightly change nearly 482cm^{-1} and 480cm^{-1} while $M-O_A-Zn(2)$, where M=Ni/K is observed around 450cm^{-1} and 444cm^{-1}. These softening of apical mode is due to variation in planer frequency of apical modes this reflects the substitution of K and Ni at Cu sites in CRL $K_{0.5}Tl_{0.5}(BaCa)O_{4-\delta}$ and $Ni_{0.5}Tl_{0.5}(BaCa)O_{4-\delta}$. Similarly when lighter atom like Mn(1.40 A^o) and Ag(1.34 A^o) is substituted in charge reservoir layer $Mn_{0.5}Tl_{0.5}(BaCa)O_{4-\delta}$ and $Ag_{0.5}Tl_{0.5}(BaCa)O_{4-\delta}$ then peak position of apical oxygen mode $Tl-O_A-Zn(2)$ and $M-O_A-Zn(2)$ where M=Ag/Mn move to high wave number. This verifies our conclusion that as the C-axis length decreases, the bond length of the apical oxygen mode decreases, allowing this mode to vibrate at a high wave number. Variation in oxygen related apical modes advises the incorporation of K, Ni, Ag and Mn in CRL.

Conclusion

$(Cu_{0.5}Tl_{0.5})Ba_2Ca_2Cu_3O_{10-\delta}$, $(Cu_{0.5}Tl_{0.5})(BaCa)(CaMg)Cu_1Zn_2O_{10-\delta}$, $(Cu_{0.5}Tl_{0.5})(BaCa)(CaMg)Zn_3O_{10-\delta}$ and $(A_yTl_{1-y})(BaCa)(CaMg)Zn_3O_{10-\delta}$ (A= Ag, K, Ni, Mn ; y=0,0.5) samples are prepared at normal pressure by employing two-steps solid state reaction method and exhibit orthorhombic crystal structure. Variations in unit cell volume and phonon modes linked to the vibrations of planar and apical oxygen atoms are softened, these findings demonstrate incorporation of Ca, Mg and Zn in the unit cell. Temperature dependence of resistivity plots exhibited suppression in Tc. Above 77K, samples $(Cu_{0.5}Tl_{0.5})(BaCa)(CaMg)Zn_3O_{10-\delta}$ without CuO2 planes showed superconducting activity. We prepared $(A_yTl_{1-y})(BaCa)(CaMg)Zn_3O_{10-\delta}$ (A=Ag, K, Ni, Mn ; y=0,0.5) types of samples to demonstrate the contribution of Cu(3d^9) atoms in superconductivity. Doping Ni, Mn, K, and Ag ions instead of Cu-atoms in the $(Cu_{0.5}Tl_{0.5})Ba_2O_{4-\delta}$ CRL totally eliminates superconductivity and results in semiconducting behavior. Theoretical prediction for the Mott-VRH mechanism is applied to measure the energy of activation for $Tl_{1.0}(BaCa)(CaMg)Zn_3O_{10-\delta}$, $Tl_{0.5}Ag_{0.5}(BaCa)(CaMg)Zn_3O_{10-\delta}$, $Tl_{0.5}K_{0.5}(BaCa)(CaMg)Zn_3O_{10-\delta}$, $Tl_{0.5}Ni_{0.5}(BaCa)(CaMg)Zn_3O_{10-\delta}$, and $Tl_{0.5}Mn_{0.5}(BaCa)(CaMg)Zn_3O_{10-\delta}$, sample having values 1.85meV, 1.41meV, 2.35meV, 2.34 meV and 6.89 meV respectively. The Lawrence and Doniach (LD) model expression were used to compute the parameters like $J_c(0)$, $B_{c(0)}$, $B_{c1(0)}$, $B_{c2(0)}$, and $\kappa = \lambda/\xi$ for $(Cu_{0.5}Tl_{0.5})Ba_2Ca_2Cu_3O_{10-\delta}$ and $(Cu_{0.5}Tl_{0.5})(BaCa)(CaMg)(Cu_{3-x}Zn_x)O_{10-\delta}$ (x = 2, 3) samples. In our samples the values of $J_c(0)$, $B_{c0}(T)$, $B_{c1}(T)$ suppress. The number of unintended defects, calculated by parameter α in samples enhanced with increasing Zn-doping, decrease in $B_{c(0)}$, $B_{c1(0)}$, $B_{c2(0)}$, $J_c(0)$ values indicate that these defects are not behaving as pinning centres shows that the London penetration depth $\lambda_{p.d}$ and the GL parameter increase in all doped samples. The Cu ($d_{x^2-y^2}$) orbital's energy is almost degenerate with that of the O (2p) orbitals in cuprates, making hybridization and hence spin fluctuation extremely strong. The energy levels of the Ni, Ag, K, Mn, and O orbitals, on the other hand, are quite different, weakening the spin fluctuations.

References

1. D. Li et al., *Nature 572*, 624 (2019)
2. A. &hilling, M. Cantoni, J.D. Guo, and H.R. Ott, Nature 362 (1993) 56.
3. Physical Properties of High Temperature Superconductors, Vol. 1-4, D.M. Ginzbetg (World Scientific, Singapore).

Loading [MathJax]/jax/output/CommonHTML/jax.js

4. H. Ihara, Phys. C 364 (2001) 289

5. A.A. Khurram, Nawazish A. Khan, J. Electromagn. Anal. Appl. 2 (2010) 63

6. C. Park, R.L. Synder, J. Am. Ceram. Soc.78 (1995) 3171.

7. H. Ihara, A. Iyo, K. Tanaka, K. Tokiwa, K. Ishida, N. Terada, M. Takumoto, Y. Sekita, T. Tsukamoto, T. Watanabe, M. Umeda,Physica C 282–287 (1997) 1973.

8. Y. Shimakawa, J.D. Jorgensen, H. Shaked, R.L. Hitterman, T. Kondo, T. Manako, Y. Kubo, Phys. Rev. B 51 (1995) 568.

9. H. Eisaki, N. Kaneko, D. L. Feng, A. Damascelli, P. K. Mang, K. M. Shen, Z. X. Shen, and M. Greven, "Effect of chemical inhomogeneity in bismuth-based copper oxide superconductors," *Phys. Rev. B*, vol. 69, p. 064512, Feb 2004.

10. P. Fulde, *Electron Correlations in molecules and solids*. Springer-V erlag Berlin Heidelberg GmbH, 1995.

11. See, for example, J. Phys. Chem. Solids, 54, No. 10 (1993)

12. SM. Quinlan, D.J. Scalapino and N. Bulut, Phys. Rev. B 49 (1994) 1470

13. D.S. Rokhsar, Phys. Rev. Lett. 70 (1993) 493.

14. R.B. Laughlin, Proc. Summer School on Modem Perspectives in Many-Body Physics, Canberra, Jan. 1993 (World Scientific, Singapore).

15. J.G. Hobor, W.J. Liverman, Y. Xu, A.R. Moodenbaugh, Phys. Rev. B 41(1990) 8757.

16. Y. Matsumoto, M. Koinuma, H. Yamamoto, T. Nishimori, Solid State Ionics 95(1997) 309–314.

17. G. Bergmann, Phys. Rep., 1984, 107, 1–58.

18. J. Ren, H. Guo, J. Pan, Y. Y. Zhang, X. Wu, H. G. Luo, S. Du, S. T. Pantelides and H. J. Gao, Nano Lett., 2014, 14, 4011–4015.

19. J. H. Chen, L. Li, W. G. Cullen, E. D. Williams and M. S. Fuhrer, Nat. Phys, 2011, 7, 535–538.

20. A. Mourachkine, High-Temperature Superconductivity in Cuprates: The Nonlinear Mechanism and Tunneling Measurements (Dordrecht, Kluwer Academic, 2002).

21. B. Keimer et al., Nature 518, 179 (2015)

22. R. Mark Wilson: Physics Today **72**, 11, 19 (2019)

23. Q.G. Luo, R.Y. Wang, J.Phys Chem Sol. 87 (1987) 90102-90108

24. Aslamazov L G and Larkin A L 1986 *Phys. Lett.* **26** 283

25. W.E.L. Doniach, in: Eizo, Kanda (Eds.), Proceedings of the Twelfth International Conference on Low Temperature Physics, Keigaku, Tokyo, 1971, p. 361.

26. S. Hikami, A.I. Larkin, Magneto resistance of high temperature superconduc tors,Mod. Phys. Lett. B 2 (1988) 693–698.

27. J. Ali, S. Hussain, N. A. Khan, A. Raza, J. Supercond. Nov. Magn, 33 (2019) 1557–1939.

28. Nawazish A. Khan, A. A. Khurram, Appl. Phys. Lett. 86, 152502 (2005).

29. A.I. Abou Aly, I.H. Ibrahim, R. Awad, A. El-Harizy, A. Khalaf, J. Supercond. Nov.Magnetism 23 (2010) 1325–1332.

30. M.P. Rojas Sarmiento, M.A. Oribe Laverde, E. Vera Lopez, D.A. Landinez, J. Roa Rojas, Conductivity, Phys. B Condens. Matter 398 (2007) 360–363.

31. J. Prade, A.D. Kulkarani, F.W. de wette, Phys. Rev. B 39 (1989) 2771.

32. A.D. Kulkarani, J. Prade, F.W. de wette, W. Kress, U. Schroder, Phys. Rev. B 40(1989) 2642.

33. W. Kress, U. Schroder, J. Prade, A.D. Kulkarani, F.W. de wette, Phys. Rev. B 38(1988) 2906.
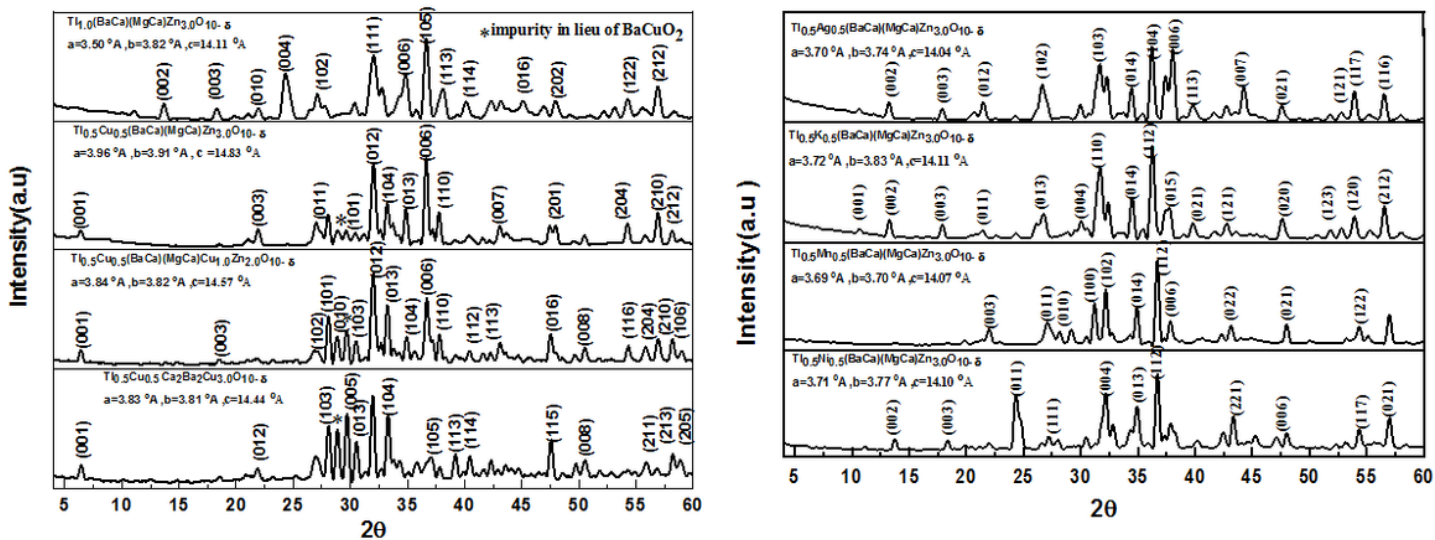
Figures

Loading [MathJax]/jax/output/CommonHTML/jax.js

Figure 1

(a) Shows XRD pattern of $(Cu_{0.5}Tl_{0.5})Ba_2Ca_2Cu_3O_{10-\delta}$, $(Cu0.5Tl0.5)(BaCa)(CaMg)Cu1Zn2O10-\delta$,$(Cu0.5Tl0.5)(BaCa)(CaMg)$ Zn3O10-δ and $(Tl1.0)(BaCa)(CaMg)$ Zn3O10-δ samples. (b) Shows XRD pattern of $(A_yTl_{1-y})(BaCa)(CaMg)$ Zn3O10-δ (A=Ag, K, Ni, Mn; y= 0,0.5) samples
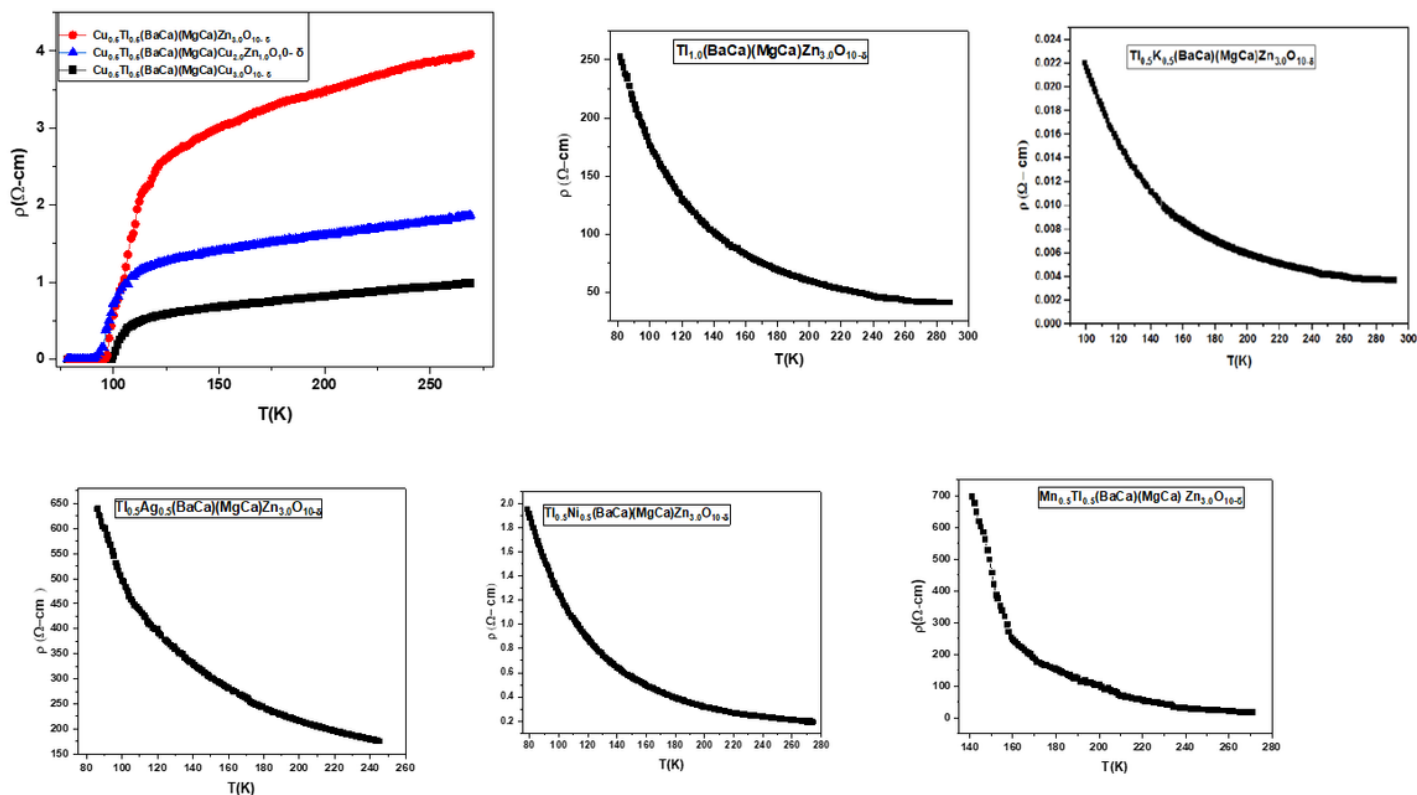
Figure 2

(a) Temperature dependence of resistivity curves of $(Cu0.5Tl0.5)Ba_2Ca_2Cu_3O_{10-\delta}$, $(Cu0.5Tl0.5)(BaCa)(CaMg)Cu1Zn2O10-\delta$, $(Cu0.5Tl0.5)(BaCa)(CaMg)$ Zn3O10-δ samples. (b,c,d,e,f) Temperature dependence of resistivity curves of $(A_yTl_{1-y})(BaCa)(CaMg)Zn3O10-(A= Ag, K; y= 0, 0.5)$ samples.
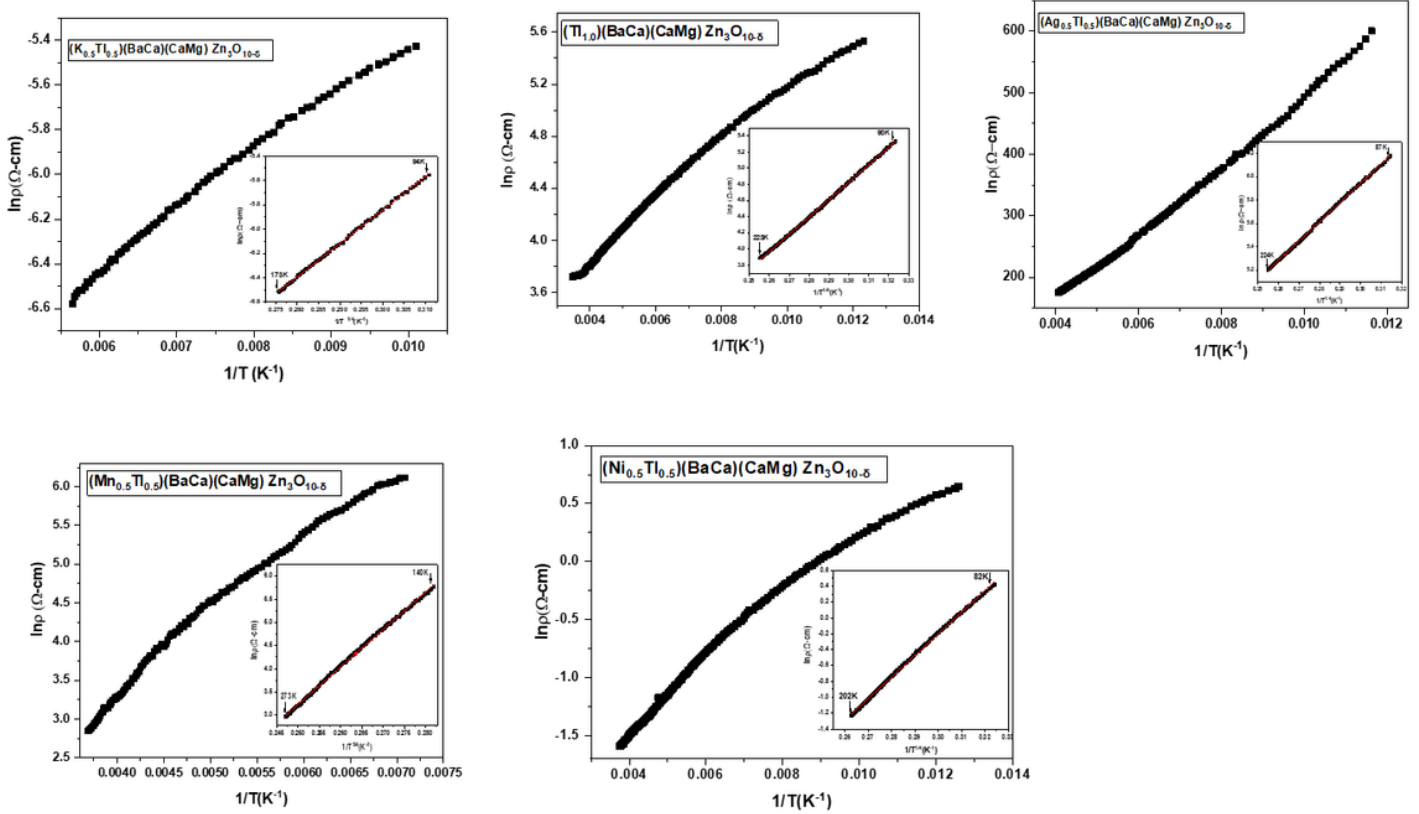
Loading [MathJax]/jax/output/CommonHTML/jax.js

Figure 3

(a,b,c,d,e) Log of Electrical resistivity (ln ρ) as a function of 1/T in the temperature range from 77K to 300K. The inset represents the plot of ln ρ vs. $1/T^{1/4}$, where the theoretical prediction for the Mott-VRH mechanism is indicated by the straight line of $(A_yTl_{1-y})(BaCa)(CaMg) Zn_3O_{10-}$ (A= Ag, K, Ni, Mn; y= 0, 0.5) samples.
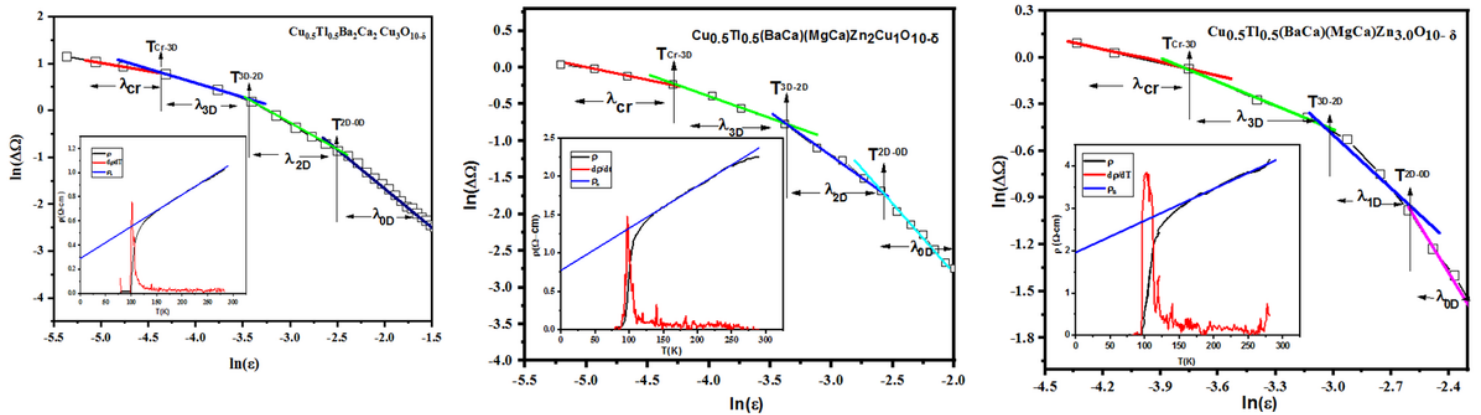

Figure 4

(a, b, c)Show the typical representation of the excess conductivity analysis of $Cu_{0.5}Tl_{0.5}Ba_2Ca_2Cu_3O_{10-\delta}$ and $Cu_{0.5}Tl_{0.5}(BaCa)(MgCa)Zn_yCu_{3-y}O_{10-\delta}$ (y = 2, 3) superconductors.
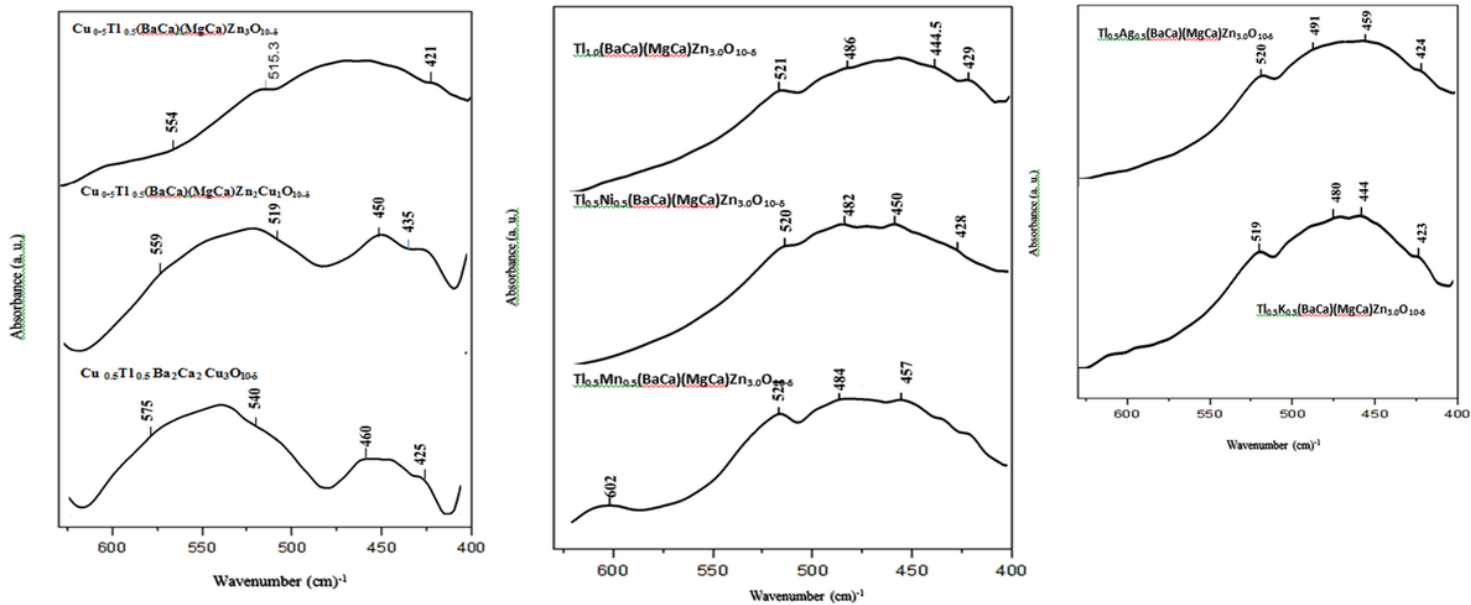
Figure 5

(a) FTIR absorbance spectrum of $(Cu0.5Tl0.5)Ba_2Ca_2Cu_3O_{10-\delta}$, $(Cu0.5Tl0.5)(BaCa)(CaMg)Cu_1Zn_2O_{10-\delta}$, $(Cu0.5Tl0.5)(BaCa)(CaMg)Zn_3O_{10-\delta}$ samples. (b) FTIR absorbance spectrum of $(Tl1)(BaCa)(CaMg)Zn_3O_{10-}$, $(Ni0.5Tl0.5)(BaCa)(CaMg)Zn_3O_{10-}$ and $(Mn0.5Tl0.5)(BaCa)(Ca\,Mg)\,Zn_3O_{10-}$ samples. (c) FTIR absorbance spectrum of $(K0.5Tl0.5)(BaCa)(Ca\,Mg)\,Zn_3O_{10-}$ and $(Ag5Tl0.5)(BaCa)(Ca\,Mg)\,Zn_3O_{10-}$ samples.